Dariusz KUSIAK[1], Zygmunt PIĄTEK[2], Tomasz SZCZEGIELNIAK[2]

Czestochowa University of Technology, Faculty of Electrical Engineering (1)
Czestochowa University of Technology, Faculty of Environmental Engineering and Protection (2)

Magnetic field in the monophase single-pole bifilar high-current busduct

Abstract. *This paper is on the determination of the magnetic field in the screen of the monophase single-pole of the bifilar high-current busduct. The components of this field have been presented by the modified Bessel functions as the functions of two variables r and Θ in the cylindrical coordinate system. These solutions take into account the magnetic field of the reverse reaction of the eddy currents induced in the screen as the result of the proximity effect and the skin effect. For each screen the distribution of the field has been shown in the function of the parameter that considers the current frequency, conductivity, and both the conductor and screen cross-dimensions. Also, it has been taken into consideration the fact that the magnetic field is the rotating elliptic and its absolute value is equal to the length of the ellipse longer axis.*

Streszczenie. *W artykule wyznaczono pole magnetyczne w ekranie jednofazowego jednobiegunowego bifilarnego toru wielkoprądowego. Składowe tego pola przedstawiano przez zmodyfikowane funkcje Bessela jako funkcje dwóch zmiennych r oraz Θ walcowego układu współrzędnych. Rozwiązania te uwzględniają pole magnetyczne oddziaływania zwrotnego prądów wirowych indukowanych w ekranie w wyniku zjawiska zbliżenia oraz zjawiska naskórkowości. Rozkłady pokazano dla każdego ekranu w funkcji parametru uwzględniającego częstotliwość prądu, konduktywność i wymiary poprzeczne przewodu i ekranu rurowego. Uwzględniono przy tym, że pole magnetyczne jest wirującym polem eliptycznym i jego moduł jest równy wartości dłuższej półosi elipsy.* ***(Pole magnetyczne w jednofazowym jednobiegunowym bifilarnym torze wielkoprądowym).***

Key words: magnetic field, tubular screen, tubular conductor, high current busduct
Słowa kluczowe: pole magnetyczne, ekran rurowy, przewód rurowy, tor wielkoprądowy

Introduction

Let us consider a magnetic field in the conducting tube-shields with the internal and external R_3 and R_4 radii, respectively, and conductivity γ_e shielding the co-axial tube-conductors of the internal and external R_1 and R_2 radii, respectively, and conductivity γ of the monophase single-pole bifilar high-current busduct with the sinusoidal current of the root-mean-square complex value - fig. 1 [1,2].

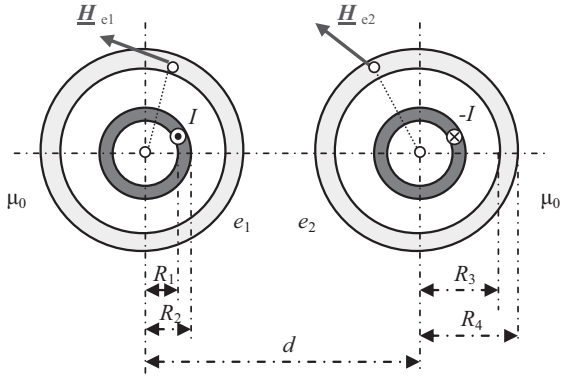

Fig. 1. Monophase single-pole high-current busduct

High current busduct shown in figure 1 is a bifilar where $\underline{I} = -\underline{I}$. Then the electromotive forces induced in the screens by magnetic fields of currents of shielded phases and adjacent phases are respectively of opposite signs and resultant electromotive force is zero. Therefore, shorting of shields or grounding on their ends will not result in flow of return currents in them [3,4,5,6].

Magnetic field in shields

The magnetic field in the first screen can be expressed as [7]

$$\underline{\boldsymbol{H}}_{e1}(r,\Theta) = \underline{\boldsymbol{H}}_{e11}(r) + \underline{\boldsymbol{H}}_{e12}(r,\Theta) = \\ = \mathbf{1}_r \underline{H}_{e1r}(r,\Theta) + \mathbf{1}_\Theta \underline{H}_{e1\Theta}(r,\Theta) \tag{1}$$

where

$$\underline{H}_{e1r}(r,\Theta) = \underline{H}_{e12r}(r,\Theta) \tag{1a}$$

and

$$\underline{H}_{e1\Theta}(r,\Theta) = \underline{H}_{e11\Theta}(r) + \underline{H}_{e12\Theta}(r,\Theta) \tag{1b}$$

In the above formulas $\underline{H}_{e12r}(r,\Theta)$ - radial component in the first screen generated by the current in the second phase, $\underline{H}_{e11\Theta}(r)$ - tangent component generated by the first phase current and $\underline{H}_{e12\Theta}(r,\Theta)$ tangent component generated in the first screen by the phase current of the second phase.

The magnetic field $\underline{\boldsymbol{H}}_{e11}(r)$ has only a tangential component, which has the form

$$\underline{H}_{e11\Theta}(r) = \frac{\underline{I}}{2\pi R_3} \underline{h}_{e11}(r) = H_{e11\Theta}(r)\, exp[j\varphi_{H\,e11\Theta}(r)] \tag{2}$$

where

$$\underline{h}_{e11}(r) = \frac{\underline{b}_0\, I_1(\underline{\Gamma}_e r) - \underline{c}_0\, K_1(\underline{\Gamma}_e r)}{\underline{d}_0} \tag{2a}$$

and

$$\underline{b}_0 = \beta_e\, K_1(\underline{\Gamma}_e R_3) - K_1(\underline{\Gamma}_e R_4) \tag{2b}$$

$$\underline{c}_0 = \beta_e\, I_1(\underline{\Gamma}_e R_3) - I_1(\underline{\Gamma}_e R_4) \tag{2c}$$

$$\underline{d}_0 = I_1(\underline{\Gamma}_e R_4)\, K_1(\underline{\Gamma}_e R_3) - I_1(\underline{\Gamma}_e R_3)\, K_1(\underline{\Gamma}_e R_4) \tag{2d}$$

and magnetic field $\underline{\boldsymbol{H}}_{e12}(r,\Theta)$ is determined from the formula

$$\underline{\boldsymbol{H}}_{e12}(r,\Theta) = -\frac{1}{\underline{\Gamma}^2} \mathbf{rot}\underline{\boldsymbol{J}}_{12}(r,\Theta) = \\ = \mathbf{1}_r \underline{H}_{e12r}(r,\Theta) + \mathbf{1}_\Theta \underline{H}_{e12\Theta}(r,\Theta) \tag{3}$$

and then its radial component has the form

$$\underline{H}_{e12r}(r,\Theta) = \frac{\underline{I}}{\pi\, \underline{\Gamma}_e\, R_4\, r} \sum_{n=1}^{\infty} \left(\frac{R_4}{d}\right)^n n\, \underline{f}_{en}(r)\, \sin n\Theta \tag{3a}$$

The tangential component is expressed then with the formula

$$\underline{H}_{e12\Theta}(r,\Theta) =$$

(3b)
$$= \frac{\underline{I}}{\pi\,\underline{\Gamma}_e\,R_4\,r}\sum_{n=1}^{\infty}\left(\frac{R_4}{d}\right)^n\left[-n\,\underline{f}_{en}(r)+\underline{g}_{en}(r)\right]cosn\Theta$$

where the function

$$\underline{f}_{en}(r) =$$

(3c)
$$= \frac{K_{n+1}(\underline{\Gamma}_e R_3)\,I_n(\underline{\Gamma}_e r)+I_{n+1}(\underline{\Gamma}_e R_3)\,K_n(\underline{\Gamma}_e r)}{I_{n-1}(\underline{\Gamma}_e R_4)\,K_{n+1}(\underline{\Gamma}_e R_3)-I_{n+1}(\underline{\Gamma}_e R_3)\,K_{n-1}(\underline{\Gamma}_e R_4)}$$

and

$$\underline{g}_{en}(r) = \underline{\Gamma}_e\,r\times$$

(3d)
$$\times\frac{K_{n+1}(\underline{\Gamma}_e R_3)\,I_{n-1}(\underline{\Gamma}_e r)-I_{n+1}(\underline{\Gamma}_e R_3)\,K_{n-1}(\underline{\Gamma}_e r)}{I_{n-1}(\underline{\Gamma}_e R_4)\,K_{n+1}(\underline{\Gamma}_e R_3)-I_{n+1}(\underline{\Gamma}_e R_3)\,K_{n-1}(\underline{\Gamma}_e R_4)}$$

The functions in the above formulas $I_n(\underline{\Gamma}_e r)$, $K_n(\underline{\Gamma}_e r)$, $I_{n+1}(\underline{\Gamma}_e R_3)$, $K_{n+1}(\underline{\Gamma}_e R_3)$, $I_{n-1}(\underline{\Gamma}_e R_4)$ and $K_{n-1}(\underline{\Gamma}_e R_4)$ are the modified Bessel functions of the firsts and second order, respectively i.e.: *n*, *n*+1 and *n*-1 [8,9,10].

In the event $\underline{I} = -\underline{I}$ relative amounts of magnetic field components in the first screen have the form

(4)
$$\underline{h}_{e1r}(\zeta,\Theta) = \frac{2}{\sqrt{2j}\,\alpha\zeta}\sum_{n=1}^{\infty}\left(\frac{1}{\lambda}\right)^n n\,\underline{f}_{en}(\zeta)\,\sin n\Theta$$

and

$$\underline{h}_{e1\Theta}(\zeta,\Theta) = \frac{1}{\beta}\underline{h}_{11\Theta}(\zeta) -$$

(4a)
$$-\frac{2}{\sqrt{2j}\,\alpha\,\zeta}\sum_{n=1}^{\infty}\left(\frac{1}{\lambda}\right)^n\left[-n\,\underline{f}_{en}(\zeta)+\underline{g}_{en}(\zeta)\right]cosn\Theta$$

where

$$\underline{f}_{en}(\zeta) =$$

(4c)
$$= \frac{K_{n+1}(\sqrt{2j}\,\alpha\beta)\,I_n(\sqrt{2j}\,\alpha\zeta)+I_{n+1}(\sqrt{2j}\,\alpha\beta)\,K_n(\sqrt{2j}\,\alpha\zeta)}{I_{n-1}(\sqrt{2j}\,\alpha)\,K_{n+1}(\sqrt{2j}\,\alpha\beta)-I_{n+1}(\sqrt{2j}\,\alpha\beta)\,K_{n-1}(\sqrt{2j}\,\alpha\beta)}$$

and

$$\underline{g}_{en}(\zeta) = \sqrt{2j}\,\alpha\zeta\times$$

(4d)
$$\times\frac{K_{n+1}(\sqrt{2j}\,\alpha\beta)\,I_{n-1}(\sqrt{2j}\,\alpha\zeta)-I_{n+1}(\sqrt{2j}\,\alpha\beta\,)\,K_{n-1}(\sqrt{2j}\,\alpha\zeta)}{I_{n-1}(\sqrt{2j}\,\alpha)\,K_{n+1}(\sqrt{2j}\,\alpha\beta)-I_{n+1}(\sqrt{2j}\,\alpha\beta)\,K_{n-1}(\sqrt{2j}\,\alpha\beta)}$$

where $\alpha = kR_4$ for $k = \sqrt{\frac{\omega\mu\gamma}{2}} = \frac{1}{\delta}$, $\beta = \frac{R_3}{R_4}$ $(0 \le \beta \le 1)$, $\lambda = \frac{d}{R_4}$ and $\xi = \frac{r}{R_4}$.

Distribution of the radial component of this magnetic field is presented in figure 2.

The magnetic field in the second screen [7]

(5)
$$\underline{\boldsymbol{H}}_{e2}(r,\Theta) = \underline{\boldsymbol{H}}_{e22}(r)+\underline{\boldsymbol{H}}_{e21}(r,\Theta) =$$
$$= \mathbf{1}_r\,\underline{H}_{e2r}(r,\Theta)+\mathbf{1}_\Theta\,\underline{H}_{e2\Theta}(r,\Theta)$$

where

(5a)
$$\underline{H}_{e2r}(r,\Theta) = \underline{H}_{e21r}(r,\Theta)$$

and

(5b)
$$\underline{H}_{e2\Theta}(r,\Theta) = \underline{H}_{e22\Theta}(r)+\underline{H}_{e21\Theta}(r,\Theta)$$

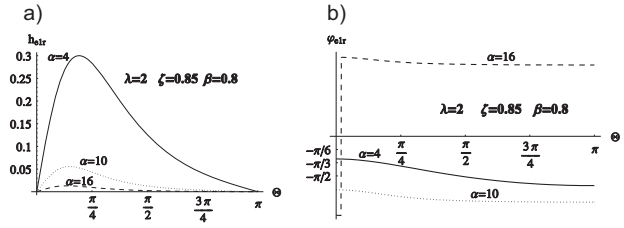

Fig. 2. Distribution of the relative values of radial component of magnetic field in the first screen of the monophase single-pole bifilar high current busduct for a fixed value of the variable ξ of: a) module, b) argument

Distribution of the radial component of this magnetic field is presented in figure 3.

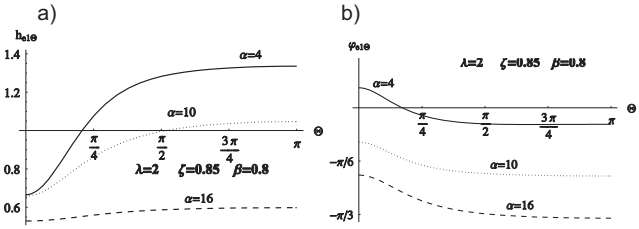

Fig. 3. Distribution of the relative values of tangential component of magnetic field in the first screen of the monophase single-pole bifilar high current busduct for a fixed value of the variable ξ of: a) module, b) argument

The magnetic field $\underline{\boldsymbol{H}}_{e22}(r)$ has only a tangential component, which is given by the formula

(6)
$$\underline{H}_{e22\Theta}(r) = -\frac{\underline{I}}{2\pi R_3}\underline{h}_{e22}(r) = H_{e22\Theta}(r)\,exp[j\varphi_{H\,e22\Theta}(r)]$$

whereas $h_{e22}(r) = \underline{h}_{e11}(r)$.

Magnetic field $\underline{\boldsymbol{H}}_{e21}(r,\Theta)$ is determined from the formula

(7)
$$\underline{\boldsymbol{H}}_{e21}(r,\Theta) = -\frac{1}{\underline{\Gamma}^2}\,\mathbf{rot}\,\underline{\boldsymbol{J}}_{21}(r,\Theta) =$$
$$= \mathbf{1}_r\,\underline{H}_{e21r}(r,\Theta)+\mathbf{1}_\Theta\,\underline{H}_{e21\Theta}(r,\Theta)$$

and then its radial component has the form

$$\underline{H}_{e21r}(r,\Theta) =$$

(7a)
$$= -\frac{\underline{I}}{\pi\,\underline{\Gamma}_e\,R_4\,r}\sum_{n=1}^{\infty}(-1)^n\left(\frac{R_4}{d}\right)^n n\,\underline{f}_{en}(r)\,\sin n\Theta$$

The tangential component is expressed then with the formula

$$\underline{H}_{e21\Theta}(r,\Theta) = -\frac{\underline{I}}{\pi\,\underline{\Gamma}_e\,R_4\,r}\times$$

(7b)
$$\times\sum_{n=1}^{\infty}(-1)^n\left(\frac{R_4}{d}\right)^n\left[-n\,\underline{f}_{en}(r)+\underline{g}_{en}(r)\right]cosn\Theta$$

In the event $\underline{I} = -\underline{I}$ relative amounts of magnetic field components in the second screen have the form

$$(8)\ \underline{h}_{e2r}(\zeta,\Theta) = -\frac{2}{\sqrt{2j}\,\alpha_c\rho}\sum_{n=1}^{\infty}(-1)^n\left(\frac{1}{\lambda_c}\right)^n \underline{f}_{en}(\zeta)\ \sin n\Theta$$

and

$$\underline{h}_{e2\Theta}(\zeta,\Theta) = -\frac{1}{\beta}\underline{h}_{22\Theta}(\zeta) +$$

$$+\frac{2}{\sqrt{2j}\,\alpha_c\rho}\sum_{n=1}^{\infty}(-1)^n\left(\frac{1}{\lambda_c}\right)^n \left[\underline{f}_{en}(\zeta)+\underline{g}_{en}(\zeta)\right] cosn\Theta \quad (8a)$$

The distribution of the total magnetic filed in the shields

Distribution of magnetic field both in the first and the second screen depends therefore on the parameter α and it is irregular distribution in regard to the angle Θ. Futhermore, the arguments of radial and tangential component of the field are different, and therefore at every point of the area tested the magnetic field is an elliptic field [11,12]. Relative module amount of this field, relative value of the longer semi-axis of field ellipse is expressed with the formula [13,14]

$$(9)\qquad h_{e1}(\zeta,\Theta) = h_1(\zeta,\Theta) + h_2(\zeta,\Theta)$$

where

$$(9a)\qquad h_1(\zeta,\Theta) = \frac{1}{2}\left|\underline{h}_{e1r}(\zeta,\Theta) + j\,\underline{h}_{e1\Theta}(\xi,\Theta)\right|$$

and

$$(9b)\qquad h_2(\zeta,\Theta) = \frac{1}{2}\left|\underline{h}^{*}_{e1r}(\zeta,\Theta) + j\,\underline{h}^{*}_{e1\Theta}(\zeta,\Theta)\right|$$

The distribution of the relative value of the magnetic field in the first and second screen in the function of the Θ angle is shown in figure 4.

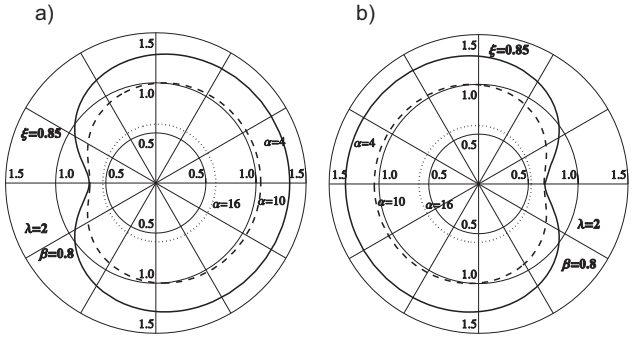

Fig. 4. The distribution of the relative value of the total magnetic field in the screen for the case $\underline{I}$ = -$\underline{I}$: a) the second screen, b) the first screen

Conclusions

The distribution of the magnetic filed in the monophase single-pole bifilar high-current busduct is uneven (figure 4), and it is due to the skin effect, but first of all due to the proximity effect consisting in pulling of the magnetic field into the system centre when currents are of opposite senses.

Introduction of relative variable ξ and parameters α, β and λ for the screen allows to show derived formulas as complex components and modules of magnetic field strength in general forms, independent of the specific values of conductivity, transverse dimensions and relative positions of the conductors and shield, and the frequency of phase currents [11]. This also allows a general analysis and visualization of modules and arguments of this field in the form of diagrams as a function of relative variables (figure 2 and 3).

As it can be seen, the modules and arguments of the complex components of the magnetic field strength are functions of two variables r and Θ of cylindrical coordinate system, and consequently, the magnetic field in this type of high-current circuits is an elliptical rotating field.

In conclusion, the skin and proximity effect strongly influences the magnetic field in this type of high current busducts, and they should be also considered for power frequency of phase currents.

REFERENCES

[1] Piątek Z.: Impedances of Tubular High Current Busducts, *Series Progress in High-Voltage technique*, Vol. 28, Polish Academy of Sciences, Committee of Electrical Engineering, *Wyd. Pol. Częst., Częstochowa* 2008.

[2] Piątek Z.: Modeling of lines, cables and high-current busducts (in Polish), Seria Monografie nr 130, Wyd. Pol. Częst., Częstochowa 2007.

[3] Piątek Z., Jabłoński P.: Foundations theory of electromagnetic fields, *WNT*, Warsaw 2010.

[4] Piątek Z., Kusiak D., Szczegielniak T.: Magnetic field in three-phase symmetrical high current busduct (in Polish), Zesz. Nauk. Pol. Śl. 2009, pp. 37-50, Elektryka, z. 1 (209).

[5] Piątek Z., Kusiak D., Szczegielniak T.: Magnetic field of double-poles high current busduct (in Polish), *Zesz. Nauk. Pol. Śl. 2009, Elektryka*, z.1(209), pp. 67-87.

[6] Nawrowski R.: High-current air or SF_6 insulated busducts (in Polish), *Wyd. Pol. Poznańskiej*, Poznań 1998.

[7] Szczegielniak T., Piątek Z.: Power Losses of the Monophase Single-Pole High-Current Busduct, Arch. of Electr. Eng. Vol.58 nr 3-4, s.107-125, 2009.

[8] Piątek Z., Kusiak D., Szczegielniak T: Magnetic field of the shielded conductor (in Polish), Przegląd Elektrotechniczny, ISSN 0033-2097, R. 85, Nr 5, 2009, ss. 92-95.

[9] Piątek Z.: Method of Calculating Total Eddy Currents Induced In Screens of a Symmetrical Three-Phase Single-Pole Gas-Insulated Transmission Line, *Acta technika CSAV*, no 53, 2008, pp. 103-120.

[10] Piątek Z.: Magnetic field in high-current isolated-phase enclosed busducts surroundings (in Polish), ZN Pol. Śl., s. Elektryka, z. 166, Gliwice 1999.

[11] Kusiak D.: Magnetic field of two- and three-pole high current busducts (in Polish), Dissertation doctor, *Pol. Częst., Wydz. Elektryczny, Częstochowa* 2008.

[12] Piątek Z.: Eddy currents inducted in the screen of the three-phase symmetrical transmission line (in Polish), *Wiadomości Elektrotechniczne*, Rok LXXVI, Nr 3/2008, ss. 17-21.

[13] Kusiak D.: Use elliptical magnetic fields in unscreened flat three phase busduct, *XXXIII IC SPETO*, Gliwice-Ustroń 2010

[14] Kusiak D.: Description of elliptic field in unshielded bifilar transmission line (in Polish), *XV Conference Computer Applications in Electrical Engineering*, ISBN 978-83-89333-34-6, Poznań 2010.

Authors: *Ph.D., Eng. Dariusz Kusiak, Institute of Industrial Electrotechnics, ul. Aleja Armii Krajowej 17, 42-200 Częstochowa,*
E-mail: dariuszkusiak@wp.pl
Prof. Ph.D., Eng. Zygmunt Piątek, Ph.D., Eng. Tomasz Szczegielniak, Institute of Environmental Engineering, ul. Brzeźnicka 60a, 42-200 Częstochowa,
E-mail: zygmunt.piatek@interia.pl, szczegielniakt@interia.pl